New Phytologist

Microbiome profiling reveals that *Pseudomonas* antagonises parasitic nodule colonisation of cheater rhizobia in *Lotus*

Duncan B. Crosbie[1], Maryam Mahmoudi[2], Viviane Radl[3], Andreas Brachmann[1], Michael Schloter[3,4], Eric Kemen[2] and Macarena Marín[1]

[1]Genetics, Biocentre, LMU Munich, Martinsried 82152, Germany; [2]Microbial Interactions in Plant Ecosystems, Centre for Plant Molecular Biology, University of Tübingen, Tübingen 72076, Germany; [3]Comparative Microbiome Analysis, Helmholtz Centre for Environmental Health, Oberschleissheim 85764, Germany; [4]Chair for Soil Science, Technical University of Munich, Freising 85354, Germany

Author for correspondence:
Macarena Marín
Email: m.marin@bio.lmu.de

Received: *22 October 2021*
Accepted: *11 January 2022*

New Phytologist (2022) **234:** 242–255
doi: 10.1111/nph.17988

Key words: ineffective nodules, *Lotus*, *Mesorhizobium*, microbiome, *Pseudomonas*, root–nodule symbiosis.

Summary

- Nodule microbiota are dominated by symbiotic nitrogen-fixing rhizobia, however, other non-rhizobial bacteria also colonise this niche. Although many of these bacteria harbour plant-growth-promoting functions, it is not clear whether these less abundant nodule colonisers impact root–nodule symbiosis.
- We assessed the relationship between the nodule microbiome and nodulation as influenced by the soil microbiome, by using a metabarcoding approach to characterise the communities inside nodules of healthy and starved *Lotus* species. A machine learning algorithm and network analyses were used to identify nodule bacteria of interest, which were re-inoculated onto plants in controlled conditions to observe their potential functionality.
- The nodule microbiome of all tested species differed according to inoculum, but only that of *Lotus burttii* varied with plant health. Amplicon sequence variants representative of *Pseudomonas* species were the most indicative non-rhizobial signatures inside healthy *L. burttii* nodules and negatively correlated with *Rhizobium* sequences. A representative *Pseudomonas* isolate co-colonised nodules infected with a beneficial *Mesorhizobium*, but not with an ineffective *Rhizobium* isolate and another even reduced the number of ineffective nodules induced on *Lotus japonicus*.
- Our results show that nodule endophytes influence the overall outcome of the root–nodule symbiosis, albeit in a plant host-specific manner.

Introduction

Leguminous plants have evolved a mutualistic interaction with nitrogen-fixing rhizobia in which the bacteria are hosted and nourished in root organs called nodules in exchange for ammonia. This so-called root–nodule symbiosis is initiated by a two-way signalling between the symbiosis partners, which activates distal cell divisions in the root cortex and culminates in the formation and infection of nodules (Venado *et al.*, 2020). Here the bacteria differentiate into plant-dependent, nitrogen-fixing endosymbiotic bacteroids (Kereszt *et al.*, 2011). The fixation of nitrogen is an energetically expensive process for the host that requires at least 16 ATP molecules per N_2 molecule to fuel the nitrogenase enzyme produced by the rhizobia (Seefeldt *et al.*, 2009). Therefore, to prevent infection of the carbon-rich nodules by pathogens, host plants have evolved complex recognition mechanisms that ensure symbiotic specificity (Wang *et al.*, 2012).

Root–nodule symbiosis is highly species specific and many plants will only form an effective symbiosis with a narrow range of rhizobia (Remigi *et al.*, 2016). Even within these pairings there is variation in nitrogen fixation efficiency (Schumpp & Deakin, 2010). Some bacteria can also nodulate plants and not fix any nitrogen at all (Sachs & Simms, 2008). Examples of ineffective nitrogen fixation have been described after the introduction of crop legumes into areas where native legumes previously grew. For instance, inefficient nitrogen fixation occurs in fields where perennial and annual clovers co-exist (Howieson *et al.*, 2005). Native rhizobial species associated with native legumes can outcompete inoculant strains (Streeter, 1994). In extreme cases, endogenous rhizobia can completely block the nodulation of introduced rhizobia. For example, the nodulation of the pea cultivars Afghanistan and Iran by rhizobial inoculants is suppressed in natural soils by the presence of a non-nodulating strain (Winarno & Lie, 1979). This suggests that interactions of the soil microbiota with the host plant are critical for the establishment of efficient nodules. However, we are far from understanding what factors determine the success of single microbes that compete for resources at the plant soil interface, in particular nodule endophytes and how these affect the outcome of the symbiosis.

There is clear evidence to suggest that the host controls the makeup of the microbiota in its vicinity. *Lotus japonicus* selects for

a broad taxonomic range of bacteria, in addition to the symbiont, within the rhizosphere, endosphere and the nodule. This selectivity filters the diverse soil microbiome into a distinct and taxonomically narrow community within the nodule (Zgadzaj *et al.*, 2016). Despite this selective pressure, nonnodulating bacteria, such as *Pseudomonas* sp., *Klebsiella* sp. and *Rhodococcus* sp. have been isolated from plant nodules (Ibáñez *et al.*, 2009; Ampomah & Huss-Danell, 2011; Martínez-Hidalgo & Hirsch, 2017). Although these isolates do not directly nodulate the plant, they contribute to plant growth in some ways, such as increasing the availability of soluble phosphate and producing plant compounds beneficial for plant growth such as siderophores and indoleacetic acid (Dey *et al.*, 2004; Malik & Sindhu, 2011; Zhao *et al.*, 2013). In addition, non-Rhizobiales microbes found in nodules of *Medicago truncatula* produce antimicrobial compounds that may shape the community and the overall function of the nodule microbiome (Hansen *et al.*, 2020). Microbe–microbe interactions could also impart an effect on the overall functionality of the symbiosis, for instance via antimicrobial activity (Tyc *et al.*, 2014), suppression of plant pathogens (Gu *et al.*, 2020) or by horizontal gene transfer (Cytryn, 2013). Although these complex interactions could dictate the effectiveness and specificity of the symbiosis, little information is known about how rhizobia interact with other members of the nodule microbiota.

In this work, we determined the nodule microbiome of three *Lotus* species upon inoculation with soil suspensions that led to the growth of either starved or healthy plants. We used metabarcoding-based high-throughput sequencing to characterise the microbiome in nodule samples that varied in plant species origin, soil inocula and plant health. Network analyses and machine learning algorithms identified microbiome members specifically associated to nodules of healthy, but not of starved *Lotus burttii* plants. Tripartite interactions between rhizobia, nodule endophytes and the host were further investigated in co-inoculation assays. Our results show that although root–nodule symbiosis is a binary interaction, there are other nodule microbes that modulate this mutualism.

Materials and Methods

Soil collection and inoculum preparation

Soil samples were collected from two neighbouring sites in a semiurban area south west of Munich, Germany. Site 1 (48°06′29.9″N, 11°27′38.9″E) has consistently been home to wild *Lotus corniculatus*, whereas site 2 (48°06′33.2″N, 11°27′41.4″ has been subjected to tilling and physical disturbance and did not contain *Lotus* plants at the time of collection. Soil samples were taken from the top layer (0–20 cm deep) after plant material was removed from the site in May 2019 and October 2018. Physicochemical property measurements of each soil were performed by AGROLAB Agrarzentrum GmbH (Landshut, Germany). Soil samples were sieved to remove stones and plant material with a 2 mm sieve, mixed 1 : 5 with a nitrogen-limiting Fabaceae (FAB) liquid medium, and stirred for 2 h. Soil particulate matter was removed by centrifugation at 1000 ***g*** for 5 min. Soil suspensions were used as inputs and a quantitative PCR (qPCR) was run to compare the quantity of soil bacteria present in both soil suspensions inputs.

Plant growth and inoculation conditions

Lotus burttii B-303 (seed bag no. 91105), *L. japonicus* Gifu B-129 (seed bag no. 110913) and *L. corniculatus* cv Leo (Andreae Saaten, Regensburg, Germany) seeds were scarified and then sterilised by incubation in a sterilising solution (1.2% NaOCl, 1% SDS) for 8 min before being washed three times with sterile water. Seeds were then soaked in sterile water for 2–3 h and germinated on 0.5 B5 agar medium (Gamborg *et al.*, 1968) for 3 d in dark followed by 3 d in a long-day photoperiod (16 h : 8 h, light : dark) at 24°C. Seedlings were then transferred into sterilised tulip-shaped Weck jars (10 seedlings per jar) containing 300 ml of a sand : vermiculite mix (1 : 2) and supplemented with 40 ml of a low nitrogen FAB medium, to create nitrogen-limiting growth conditions as mentioned above (Liang *et al.*, 2019). Jars were sealed with micropore tape to create a closed system. Seedlings were left to recover for 2 d in a long-day photoperiod. After the 2-d recovery, each seedling was inoculated with 1 ml of soil suspension. *Lotus burttii* and *L. japonicus* treatments consisted of 150 plants from three independent experiments, and *L. corniculatus* treatments consisted of 50 plants per condition from one independent experiment.

Harvesting, phenotyping and nodule surface sterilisation

Plants were harvested and phenotyped 5 wk post inoculation across five independent experiments. Shoot length, shoot dry weight, nodule number, nodule colour and plant health were recorded. Nodules were classified as pink or white, which indicated the presence or absence of leghaemoglobin, respectively, a prerequisite for, but not a guarantee of, nitrogen fixation (Downie, 2005). Roots were removed from shoots and sonicated using the Bioruptor® (Diagenode, Seraing, Belgium) twice for 15 min. Nodules from three or four plants were excised and pooled based on similarity of plant shoot and nodule phenotype. Pink and white nodules were collected separately. Pooled nodules were treated with 70% ethanol for 1 min followed by 2% NaOCl for 2.5 min. Nodules were then washed with sterile water eight times and after the removal of the final water wash, samples were snap frozen in liquid nitrogen. The final wash was plated onto 20Q agar supplemented with 3.8% w/v mannitol (modified from Werner *et al.*, 1975) to assess sterilisation.

DNA extraction

Nodule samples were homogenised six times in a Mixer Mill 400 (Retsch, Haan, Germany) at a frequency of 30 s^{-1} for 1 min. DNA was then extracted according to a modified protocol from Töwe *et al.* (2011). For extraction of DNA from the inputs, soil suspensions were centrifuged at 5000 ***g*** and DNA from pellets was extracted according to the CTAB method described by the Doe Joint Genomics Institute (William *et al.*, 2012). The

concentrations of extracted DNA samples were quantified using a Qubit 2.0® fluorometer (Invitrogen, Carlsbad, CA, USA).

Quantitative PCR

Quantitative PCR was performed using the forward primer (FP) *16S rDNA* (5′-GGTAGTCYAYGCMSTAAACG-3′) and reverse primer (RP) *16S rDNA* (5′-GACARCCATGCASCACCTG-3′) primers (Bach *et al.*, 2002). The 25-µl PCR mixture contained 12.5 µl SYBR Green, 2 µl template DNA, 7.5 µl Milli-Q water, 1 µl 10 µM of primers and 1 µl 15% bovine serum albumin (BSA). The mixture was amplified using a CFX96 Real-Time System (Bio-Rad, Hercules, CA, USA) under the following conditions: template was denatured at 94°C for 10 min before 40 cycles of 95°C for 20 s, 57°C for 30 s and 72°C for 45 s, followed by dissociation curve steps of 95°C for 15 s, 60°C for 30 s and 95°C for 15 s. Quantification of the *16S* rRNA gene molecules was correlated with a calibration curve constructed with known amounts of a *16S* rRNA gene standard plasmid constructed of a *Mesorhizobium septentrionale 16S* rRNA gene sequence cloned into a pUC57 plasmid.

Amplification, library preparation and sequencing

To determine bacterial diversity, a metabarcoding approach was utilised. The hypervariable region V3–V4 of the *16S* rRNA gene was amplified using universal bacterial primers 335F (5′-CADACTCCTACGGGAGGC-3′) and 769R (5′-ATCCTGTTTGMTMCCCVCRC-3′) fused to Illumina adapters. The primers were specific for bacterial DNA and did not amplify plastidial and mitochondrial plant DNA (Dorn-In *et al.*, 2015). Amplification reaction volumes were 25 µl using 1 unit of Phusion polymerase, 5 µl 5× High-Fidelity Phusion buffer, 7.5 µl of 1% BSA, 0.5 µl of 10 mM dNTPs, 0.5 µl of 50 mM $MgCl_2$, 0.5 µl of 10 pmol μl^{-1} primer and 5 ng of template DNA. The assay was conducted in triplicate under the following conditions: template was denatured at 98°C for 1 min, then 25 cycles of 98°C for 10 s, 55°C for 30 s and 72°C for 30 s, followed by a final step at 72°C for 5 min. PCR products were verified via gel electrophoresis, pooled, and cleaned using CleanPCR beads (CleanNA, Waddinxveen, the Netherlands). Fragments were then indexed with 10 nucleotide barcode sequences using the Nextera XT Index Kit v.2 Set D primers (Illumina, San Diego, CA, USA). Indexing PCR reactions were run in triplicate with a volume of 25 µl using 12.5 µl NEB Next High-Fidelity Master Mix, 2.5 µl of each delegated primer and 20 ng of amplicon under the following conditions: template was denatured at 98°C for 30 s, then eight cycles of 98°C for 10 s, 55°C for 30 s and 72°C for 30 s, followed by a final step at 72°C for 5 min. PCR products were pooled and cleaned with CleanPCR beads (CleanNA). Quantification and quality control were conducted using an AATI Fragment Analyser (Santa Clara, CA, USA). All samples were pooled at an equimolar concentration for paired-end 2 × 300-bp sequencing via the MiSeq system (Illumina) using the MiSeq Reagent Kit v.3 (600 cycles), as per the manufacturer's recommendation.

Sequence and statistical analysis

An average of *c.* 141 000 raw Illumina reads per sample were obtained, which were then demultiplexed and had adapter and barcode sequences removed using CUTADAPT v.3.1 (Martin, 2011). Reads were then trimmed, merged and filtered using DADA2 (Callahan *et al.*, 2016) in R. The criteria for filtering were minimum lengths of 280 bp for the forward reads and 160 bp for the reverse, as these lengths corresponded to a minimum quality score of 25. Merged sequences had chimeras and chloroplastic and mitochondrial sequences removed. Amplicon sequence variants (ASVs) were assigned in R using the Silva database v.132 (Quast *et al.*, 2012).

The PHYLOSEQ v.1.26.1 package in the R (McMurdie & Holmes, 2013) pipeline was used to infer alpha diversity of ASVs rarefied corresponding to the sample with the lowest number of reads. Multidimensional Scaling using Bray–Curtis (Bray & Curtis, 1957) distance was performed using the PHYLOSEQ v.1.26.1 package in R (McMurdie & Holmes, 2013) to assess the beta diversity of microbial communities. Comparisons were visualised using GGPLOT2 (Wickham, 2009) in R and tested for statistical significance (*adonis* test, $P < 0.01$) via permutational multivariate analysis of variance (PERMANOVA) utilising 999 permutations in the VEGAN package (Oksanen *et al.*, 2018). Relative abundance of each genera per sample was calculated using transformed count data. To further specify the composition of the sample microbiome the relative abundance of the most prevalent ASVs (abundance > 0.1%) was calculated for each sample. All abundance levels were calculated using the PHYLOSEQ v.1.26.1 package (McMurdie & Holmes, 2013) in R.

Machine learning model

A support vector machine learning model by svm.SVC (kernel=linear) in PYTHON SCIKIT-LEARN (Pedregosa *et al.*, 2011) was used to discriminate between starved and healthy plant samples of *L. burttii* on relative abundance filtered ASVs using five-fold cross-validation. The ASV tables were filtered to ASVs present at ≥ 50 reads in soil suspension 2 inoculated *L. burttii* nodule samples. The *svm.SVC.coef* function was used to calculate the coefficient value of the ASVs. These values were then used to identify signature ASVs characteristic of certain sample types. The model was trained with 70% of the data and evaluated by 30% of the data five times (mean of accuracy = 0.89) with the average coefficient value of each ASV being used to select for important features.

Microbial correlation networks

Filtered ASV tables comprised of samples of *L. burttii* inoculated with soil suspension 2 (ASV raw abundances) were used to calculate microbial correlation networks among ASVs using the SPARCC (Friedman & Alm, 2012) algorithm in FASTSPAR (Watts *et al.*, 2019). This algorithm uses log-ratio variances of ASV fractions to calculate pairwise correlations between ASVs in an iterative manner. The filtered tables were used to calculate the

correlation between ASVs using the FastSpar implementation and the default parameters. Pseudo *P*-values were inferred from 1000 bootstraps. Only correlations with $P < 0.01$ were kept for further analyses. Network visualisation was performed in Cytoscope v.3.8.2 (Shannon *et al.*, 2003). Analysis of interactions between and within ASVs of different genera were carried out using the same methods.

Isolation of strains

Strains were isolated from crushed nodules on a variety of media. Nodules from either *L. burttii*, *L. corniculatus* or *L. japonicus* inoculated with either soil suspension 1 or 2 were sterilised as described above (see 'Harvesting and nodule sterilisation' in the Materials and Methods section). Individual nodules were crushed in 10 mM $MgSO_4$ and the content was then spread onto 20Q agar plates supplemented with mannitol, lysogeny broth (LB) (Bertani, 1951), yeast mannitol (YM) (Vincent, 1970), *Pseudomonas* minimal medium (PMM) (Sandman & Ecker, 2014), and tryptone soy (TS) (Sigma, Darmstadt, Germany). Plates were incubated at 28°C for up to 3 wk and further isolation of single colonies was carried out 7–9 times until pure cultures were attained. The taxonomy of each strain was determined by amplifying the *16S* rRNA gene using primers 41f (5′-GCTCAGATTGAACGCTGGCG-3′) and 1488r (5′-CGGTTACCTTGTTACGACTTCACC-3′) (Herrera-Cervera *et al.*, 1999) and Phusion polymerase. Amplicons were purified using a 1 : 0.8 ratio of PCR product to CleanPCR beads (CleanNA) and sequenced using *16S* rRNA gene-specific primers, 41f and 1488r (Herrera-Cervera *et al.*, 1999), by Sanger sequencing. Sequences were aligned to DNA sequences from the NCBI Nucleotide collection online database using Blastn (Altschul *et al.*, 1990). The sequences of the isolates were aligned with ASV sequences using CLC Main Workbench 7 (Qiagen, Hilden, Germany). Strains were stored in 40% glycerol at −80°C.

Isolate inoculations

Bacteria were streaked and grown until single colonies formed. Single colonies were inoculated into 2 ml of the appropriate liquid medium and grown at 28°C for 2, 3 or 5 d for *Pseudomonas* sp. strains, *Rhizobium* sp. BW8-2 and *Mesorhizobium* sp. Qb1E3-1, respectively. Bacteria were then washed in sterile water and resuspended in FAB medium to allow for a final OD_{600} of 0.005. Each plant was inoculated with 1 ml of bacterial suspension. Plants were prepared as described above.

Conjugation

Strains used in this work are listed in Supporting Information Table S1. *Escherichia coli* ST18 transformed with pFAJ-GFP and pFAJ-*Ds*Red plasmids (Kelly *et al.*, 2013) and *E. coli* S17.1 transformed with pABC-Cerulean were grown at 37°C overnight in LB supplemented with appropriate antibiotics. *Pseudomonas* sp. Lb2C2, *Rhizobium* sp. BW8-2 and *Mesorhizobium* sp. Qb1E3-1 were grown at 28°C in 20Q liquid with the appropriate antibiotics for 2, 3 and 5 d, respectively. Conjugations were conducted as in Liang *et al.* (2019). Successful conjugation was confirmed via fluorescence microscopy and *16S* rRNA gene sequencing.

Section preparation and microscopy

Lotus burttii seeds were sterilised, germinated, potted and inoculated with fluorescent strains as described above (see 'Plant growth and inoculation conditions' and 'Isolate inoculations' in the Materials and Methods section). Plants were harvested 2 wk after inoculation and the nodules were excised and embedded in 6% low melting agarose. The nodules were then sliced into 100 µm-thick sections using a VT1000S vibratome (Leica Biosystems, Wetzlar, Germany) and visualised with a TCS SP5 confocal microscope (Leica Microsystems, Wetzlar, Germany) equipped with a ×20 HCX PL APO water immersion lens. GFP and Cerulean were excited with an argon laser line at 488 and 433 nm, and the emissions were detected at 492–515 and 455–474 nm, respectively. *Ds*Red was excited with a diode pumped solid-state laser at 561 nm and detected at 580–620 nm.

Statistical analyses

The nodule and root phenotype of plants inoculated with nodule isolates were recorded. Statistical significance was assessed using analysis of variance (ANOVA) and Tukey honestly significant difference (HSD) tests in R (Graves *et al.*, 2015).

Results

Species-specific effect of soil inoculum on *Lotus* plant growth

Two different soil suspensions were used to inoculate *L. burttii*, *L. japonicus*, and *L. corniculatus* plants. These *Lotus* species were selected as they all belonged to the *L. corniculatus* clade (Kramina *et al.*, 2016), but nodulated with a different range of microsymbionts (Gossmann *et al.*, 2012; Sandal *et al.*, 2012). The first soil (soil 1) was collected at a site that contained healthy wild growing *L. corniculatus* plants, while the second soil (soil 2) site contained no leguminous plants at all. The soils had minor differences in mineral content and grain size (Table S2). The quantity of soil bacteria present in the soil suspensions used as inputs was compared by qPCR. Soil suspension inputs 1 and 2 contained 1.62×10^5 and 2.28×10^5 molecules of the *16S* rRNA gene per nanogram of extracted DNA, respectively.

Lotus japonicus, *L. burttii* and, to a lesser extent, *L. corniculatus*, produced exclusively healthy plants (green leaves, elongated shoots) when inoculated with soil 1 suspension (Soil S1; Fig. 1). Contrastingly, there was marked variation in the shoot growth phenotype seen in all species when inoculated with the soil 2 suspension (Soil S2). Growing alongside the healthy plants was a large contingent of starved plants presenting with shorter shoots and yellow leaves (Fig. 1). Similar results were observed across five independent experiments (Fig. S1). Nodule number also varied dependent on soil suspension inoculum. Plants inoculated with soil 1 suspension

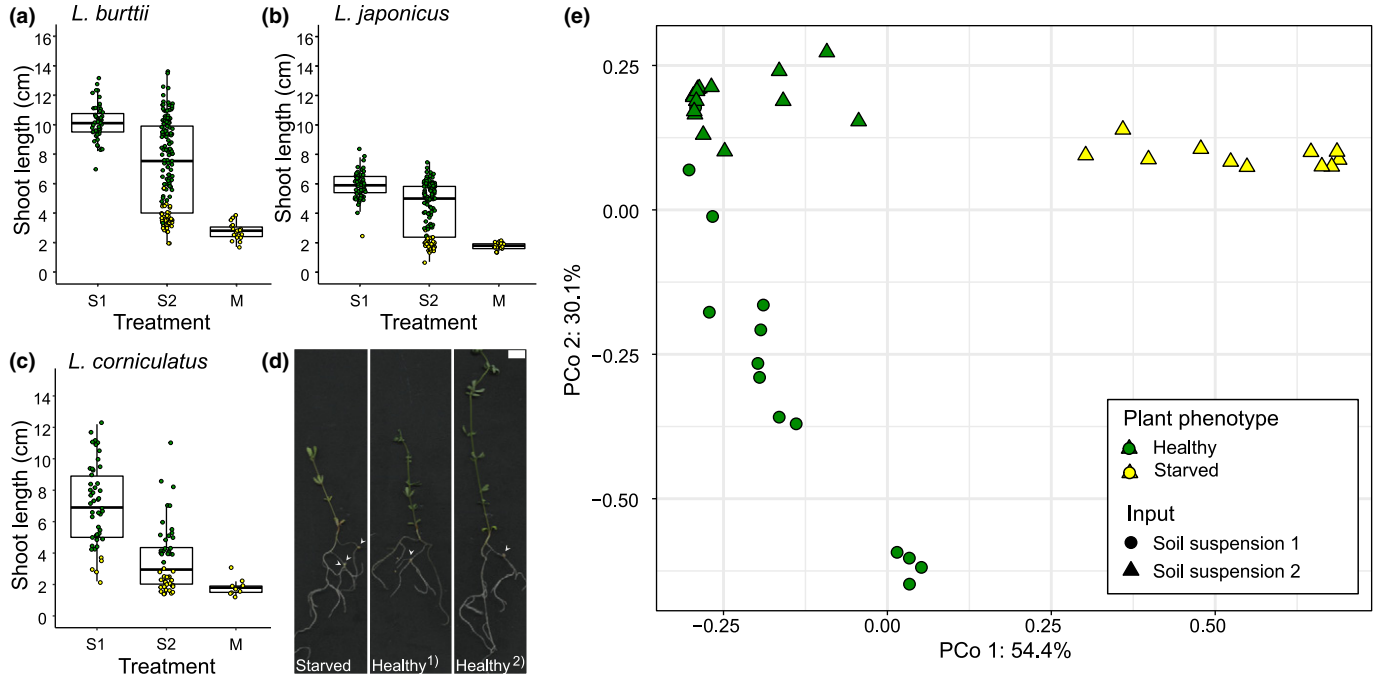

Fig. 1 Shoot growth phenotype of *Lotus* plants inoculated with Munich soil suspensions. Shoot growth quantification of *Lotus burttii* (a), *Lotus japonicus* (b) and *Lotus corniculatus* (c) plants 5 wk post inoculation with soil suspensions 1 (S1) and 2 (S2) and a mock (M) treatment. Green and yellow dots indicate plants with healthy and starved phenotypes, respectively. Box plots display the results of 50–150 plants per condition. The bold black line and the box depict the median and the interquartile range, respectively. In total, 49 mock treated plants were included. (d) Scanned images of *L. burttii* 5-wk post inoculation with soil suspension 2. Starved plants exhibited pale green leaves despite having nodules on their roots. The shoots of healthy dark green plants varied in length. Phenotypic variation is depicted in [1)] and [2)]. White arrowheads indicate the position of nodules on plant roots. Plots show the results from one representative experiment. Bar, 1 cm. (e) Principal coordinates analysis plot of *L. burttii* nodules based on beta diversity calculated using the Bray–Curtis dissimilarity index (Bray & Curtis, 1957) revealed a clustering of common sample types and a separation of dissimilar sample types.

consistently developed a higher number of nodules per plant across all species (Fig. S2a–c). Starved plants inoculated with the soil 2 suspension exhibited roots either with or without nodules. In *L. burttii*, 73.8% of starved plants contained nodules, while in *L. japonicus* and *L. corniculatus*, 45.2% and 59.3% exhibited nodules, respectively (Fig. S2d). However, the most striking difference was that in *L. burttii* 88.4% of the nodules on starved-nodulated plants were white, whereas in the other species most of the nodules were pink (Fig. S2e). These results showed that the microbiota of the soil 2 suspension is capable of mediating both effective and ineffective symbiosis, although the frequency at which each plant succumbs to an ineffective nodulation differs.

Richness, diversity and community structure of the *Lotus* nodule microbiome

The microbiome of an effective plant nodule is typically dominated by the respective symbiont, although there can also be colonisation by other microbes (Martínez-Hidalgo & Hirsch, 2017). To investigate how the nodule microbiota varied depending on the plant host, inoculum, and nodule phenotype we sequenced the microbiome of nodules collected from healthy and starved *Lotus* of different species inoculated with different soil suspensions. A variable region of the *16S* rRNA gene was sequenced and the output reads were processed, sorted into ASVs and assigned a taxonomy. ASVs were used as they provide a finer resolution than Operational Taxonomic Units (Callahan *et al.*, 2017), which is important as the 16S rRNA gene of some rhizobia, such as *Mesorhizobium*, can be more than 99% identical between different species (Marcos-García *et al.*, 2015). Sequencing produced 13 989 700 paired-end reads after quality filtering, which clustered into 67 442 unique ASVs. Sequence coverage varied between sample types with the nodule samples having an average of 148 679 reads per sample and the soil suspension input samples having an average of 67 618 reads per sample (Dataset S1). All rarefaction curves reached a saturation plateau (Fig. S3).

To assess the effect of the host genotype and the inoculum on the nodule microbiome diversity, the alpha and beta diversities of the different nodule samples from all three species were determined. Within sample variation (alpha diversity) was calculated using the Shannon diversity index, which was found to be much higher in the soil suspension input samples compared with the nodule samples (Fig. S4a). The soil suspensions 1 and 2 did not significantly vary in their alpha diversities (Welch two sample *t*-test, $P = 0.749$), although it was found that plants inoculated with soil 1 suspension produced nodules with a much higher alpha diversity compared with those inoculated with soil 2 suspension. This observation was most pronounced in *L. japonicus* and *L. corniculatus* (Fig. S4). A similar trend in alpha diversity was seen when considering observed ASVs (Fig. S4b).

To analyse the diversity between sample types (beta diversity), principal coordinate and PERMANOVA analyses were conducted using the Bray–Curtis dissimilarity. A global comparison of the nodule diversity showed an overall separation based on soil suspension input (Fig. S5; Soil S1 vs Soil S2, $Pr(>F) = 0.001$; Table S3), despite the two soil suspension inputs showing insignificant differences between one another (Soil S1 vs Soil S2 (input suspension), $Pr(>F) = 0.072$; Table S3). The most pronounced difference was between nodules of *L. burttii* plants. At the species level, *L. burttii* and *L. japonicus* showed a significant difference in beta diversity based on soil suspension input (*Lb* healthy plants – Soil S1 vs Soil S2, $Pr(>F) = 0.001$; *Lj* healthy plants – Soil S1 vs Soil S2, $Pr(>F) = 0.002$; Table S3). *Lotus burttii* nodules showed a significant difference in beta diversity based on plant health (*Lb* Soil S2 – healthy vs starved plants, $Pr(>F) = 0.001$; Fig. 1d; Table S3), however this was not the case in *L. japonicus* or *L. corniculatus* (*Lj* Soil S2 – healthy vs starved plants, $Pr(>F) = 0.097$; *Lc* Soil S2 – healthy vs starved plants, $Pr(>F) = 0.742$; Table S3). As a control, we compared the microbiome of laboratory grown *L. corniculatus* plants to the microbiome of nodules collected from *L. corniculatus* plants growing on site 1 (*Lc* Soil S1 – laboratory grown vs wild plants, $Pr(>F) = 0.342$) (Table S3). These did not significantly differ, supporting that nodules produced in this growth/inoculation system are representative of nodules grown in the wild.

Bacterial composition of the nodule microbiome

Both soil suspension types were dominated by Alphaproteobacteria and Gammaproteobacteria. To determine the bacterial composition of the nodule microbiome we estimated the relative abundance at an ASV level. The nodule microbiome of all *Lotus* species was dominated by ASVs belonging to the order Rhizobiales. Nodules of healthy plants were largely dominated by *Mesorhizobium*, independent of the host and soil suspension input. However, while nodules from plants inoculated with soil 1 suspension were colonised with a variety of different *Mesorhizobium* ASVs, the nodules of healthy plants inoculated with soil 2 suspension were almost exclusively colonised by *Mesorhizobium* ASV1 (Fig. 2). This disparity in *Mesorhizobium* ASV presence is despite the observation that there is no significant difference between the *Mesorhizobium* ASVs present in the two suspensions (*Meso.* Soil S1 vs *Meso.* Soil S2, $P(>F) = 0.479$). Nodules of starved *L. burttii* plants were largely colonised by bacteria belonging to what was taxonomically defined as *Allorhizobium–Neorhizobium–Pararhizobium–Rhizobium* and will be referred to as *Rhizobium* (Fig. 2a). This suggests that *L. burttii* plants are less selective compared with *L. corniculatus* and *L. japonicus* and develop an ineffective symbiosis with *Rhizobium* strains.

Pseudomonas are more prevalent in healthy plant nodules and negatively correlate with ineffective *Rhizobium*

Support Vector Machine (SVM) is a machine learning method used to separate a data set using a linear or nonlinear surface (Noble, 2006). In this instance we used a linear-kernel to transform the data and then based on this transformation defined a boundary separating data points, ASVs, based on the nodule phenotype of *L. burttii* plants inoculated with soil 2 suspension. The SVM model revealed that *Mesorhizobium* ASV 1 (M.1) was by far the most dominant indicator of a healthy nodule (Fig. 3), which is not surprising as *Mesorhizobium* is the typical symbiont of *L. burttii* (Rodpothong *et al.*, 2009). The second two most influential indicators of a healthy microbiome were *Pseudomonas* ASVs 28 and 57 (P.28 and P.57), which were present in both soil suspension inputs. The three ASVs most indicative of a starved *L. burttii* nodule microbiome were *Rhizobium* ASVs. Once we had identified the genera most characteristic of healthy and starved *L. burttii* nodules we wanted to predict how they interacted. A microbial network was constructed with soil suspension 2 inoculated *L. burttii* samples by using SparCC (Friedman & Alm, 2012) which analysed interactions between and within ASVs from different genera (Figs 4, S6). The ratios of negative to positive interactions within *Rhizobium* and *Mesorhizobium* ASVs were 1.13 and 1.05, respectively. *Pseudomonas* ASVs all correlated positively with one another (number of edges = 8). The ratio of negative to positive interactions between *Rhizobium* and *Mesorhizobium* (ratio = 1.64) was higher compared with this ratio among *Pseudomonas* and *Mesorhizobium* (ratio = 0.77), indicating that symbiotically beneficial *Mesorhizobium* ASVs co-occur with *Pseudomonas*. Strikingly, between *Pseudomonas* and *Rhizobium* ASVs, all correlations were negative (number of edges = 37) also supporting the SVM analysis, which showed that these ASVs were characteristic of healthy and starved *L. burttii* nodules, respectively.

Pseudomonas isolate co-colonises *Mesorhizobium* but not *Rhizobium*-induced nodules

To validate sequencing data, we inoculated *Lotus* plants with bacterial strains isolated from *Lotus* nodules (Table S1). To determine the nodule colonisation pattern of *Pseudomonas* sp. PLb11B, we co-inoculated a fluorescently tagged strain with either *Mesorhizobium* sp. Qb1E3-1, which induces effective nodules or *Rhizobium* sp. BW8-2, which induces ineffective nodules, onto *L. burttii*. Fluorescence microscopy revealed that 32.5% (14/43) of nodules induced by *Mesorhizobium* sp. Qb1E3-1 contained *Pseudomonas* sp. PLb11B. The *Pseudomonas* nodule colonisation was intracellular and was confined to particular areas of the nodule, only infecting a minority of nodule cells (Fig. 5). Conversely no plant nodules (0/22) induced by *Rhizobium* sp. BW8-2 contained *Pseudomonas* sp. PLb11B after a co-inoculation (Fig. 5).

Co-inoculation of a *Pseudomonas* isolate decreases ineffective nodulation by a *Rhizobium* but not a *Mesorhizobium* isolate in a species-specific manner

To investigate if the negative correlation between *Pseudomonas* and *Rhizobium* ASVs in nodules underlay an antagonistic interaction, *Lotus* plants were co-inoculated with nodule isolates *Pseudomonas* sp. Lb2C2 and *Rhizobium* sp. BW8-2 representing the

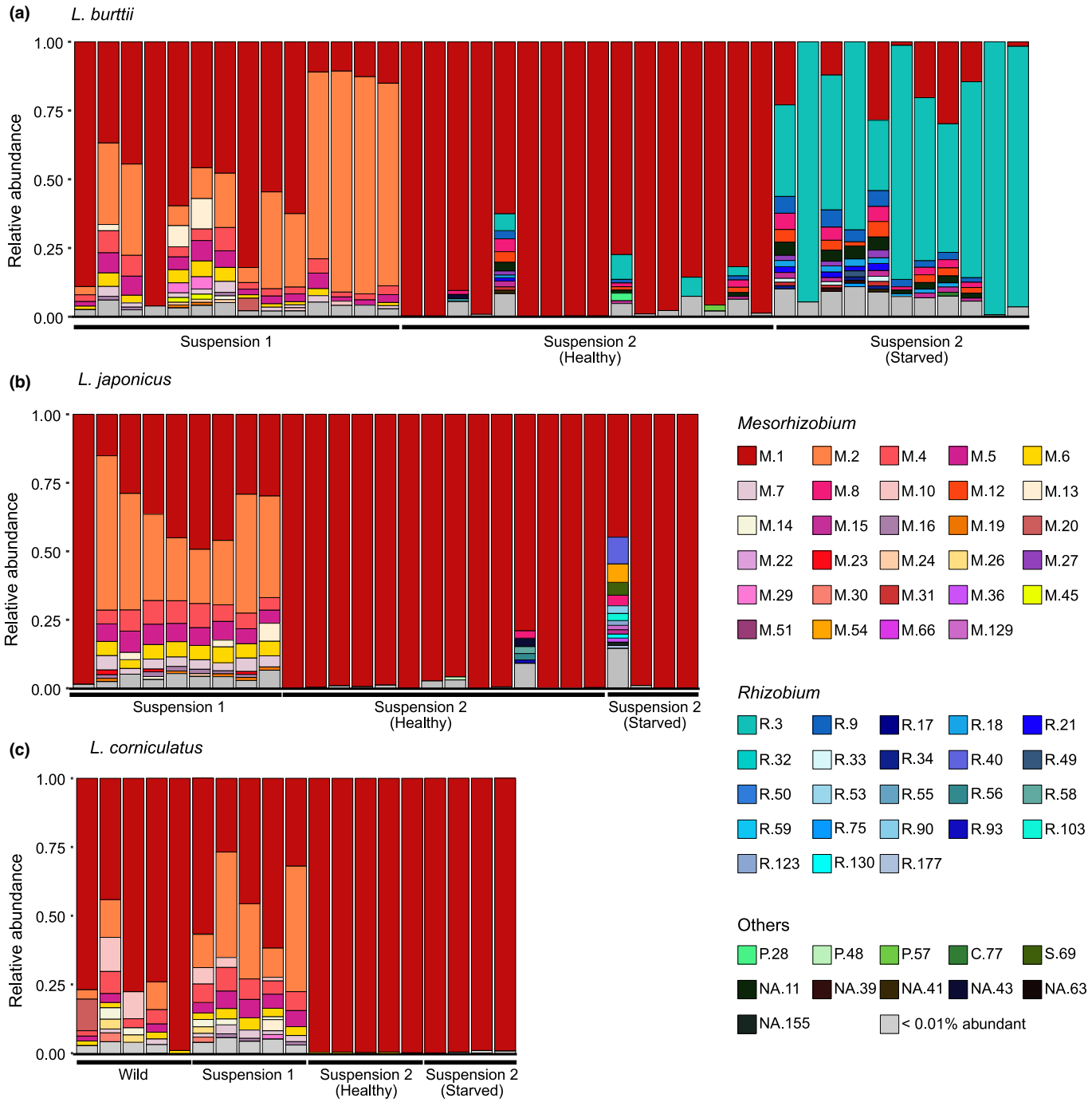

Fig. 2 Community profile showing the relative abundance of amplicon sequence variants (ASVs) present in *Lotus* nodules. The relative abundance of ASVs was estimated for *Lotus burttii* (a), *Lotus japonicus* (b) and *Lotus corniculatus* (c) using transformed data and the PHYLOSEQ v.1.26.1 package in R (McMurdie & Holmes, 2013). *Mesorhizobium* (M) ASVs are depicted in red, yellow, orange, pink and purple shades, *Rhizobium* (R) ASVs are depicted in cyan and blue shades. Other ASVs are depicted in green and black. Amplicon sequence variants < 0.01% abundant are coloured grey. NA, not assigned (taxonomy could only be defined to a Family level).

ASVs in question. *Rhizobium* sp. BW8-2 induced a large number of ineffective nodules and nodule primordia on the roots of *L. japonicus*. Co-inoculation with Lb2C2 significantly decreased the number of nodule structures (Fig. 6). No significant difference was observed regarding root weight and shoot length (Fig. S7). This inhibitory effect was host specific, as no variation in nodule number was observed in *L. burttii* upon co-inoculation with BW8-2 and Lb2C2. By contrast, co-inoculation of Lb2C2 with the effective symbiont *Mesorhizobium* sp. Qb1E3-1 saw no reduction in the nodulation of *L. burttii* or *L. japonicus* (Fig. 6) and only minimal variation in shoot length and root weight (Fig. S7). Inoculation with all three strains did not induce a

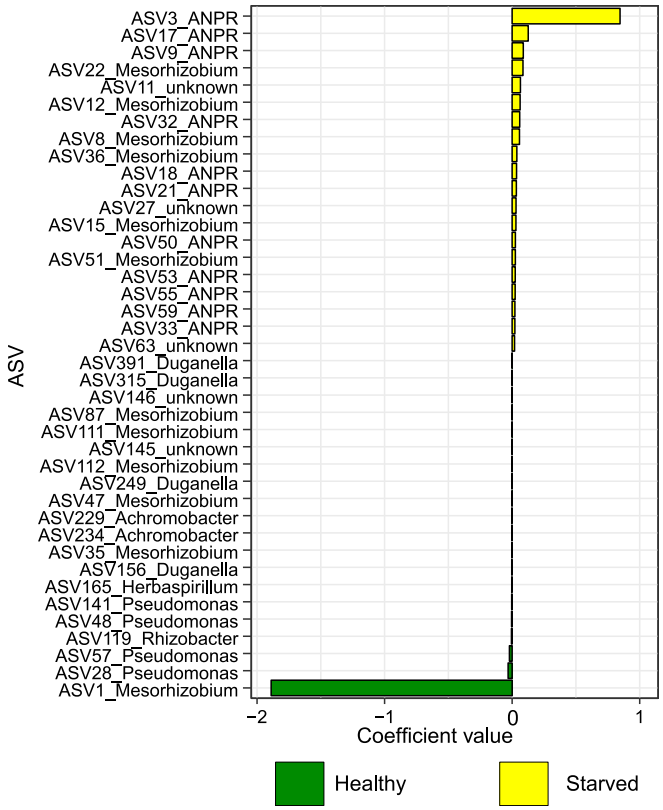

Fig. 3 Indicator amplicon sequence variants (ASVs) of samples. Support Vector Machine linear model from SCIKIT-LEARN packages were used to identify separator ASVs between healthy and starved *Lotus burttii* plants inoculated with soil 2 suspension. Histogram represents the coefficient scores of top 20 ASVs form healthy and starved plants. Negative coefficient values (green bars) represent indicator ASVs in healthy plants while positive values (yellow bars) show indicator ASVs in starved samples. The family of representative ASVs are shown after the ASV number with 'ANPR' indicating *Rhizobium* and 'unknown' indicating that no taxonomy could be assigned at a species level (NA).

different phenotype compared with co-inoculations with *Mesorhizobium* sp. Qb1E3-1 and *Rhizobium* sp. BW8-2 (Fig. S8).

Discussion

Nodules of legumes are not only colonised by rhizobia. Despite this, little information is known about how microbes other than rhizobia affect the root–nodule symbiosis, in particular nodule function and plant health. Here, we characterised variation in the bacterial microbiome of nodules dependent on plant species and soil suspension inoculum and determined correlations between the microbiome makeup and plant health using *16S* rRNA gene amplicon sequencing. Our study revealed that (1) the nodule microbiome of *L. japonicus*, *L. corniculatus* and *L. burttii* is dependent on soil suspension inoculum, (2) the nodule microbiome of starved *L. burttii* plants differs from that of the healthy plants, (3) *Pseudomonas* strains are more prevalent in healthy plant nodules than in starved-plant nodules; co-colonise effective nodules; and reduce the formation of ineffective nodules in a host-specific manner.

Soil suspension input influences *Lotus* spp. nodule microbiome

The nodule microbiome of *Lotus* plants is dependent on the soil suspension inoculum (Fig. S5; Table S3). Soil is the main influencing factor on the rhizosphere, root or nodule microbiomes in nonlegumes (Simonin *et al.*, 2020; Thiergart *et al.*, 2020) and legumes such as *M. truncatula* (Brown *et al.*, 2020) and soybean (Liu *et al.*, 2019; Han *et al.*, 2020). However, many of these studies cite the vast differences in the diversity of the microbial communities or the physicochemical properties of the soil suspension inputs as the reason for the disparity in plant microbiomes (Brown *et al.*, 2020; Han *et al.*, 2020; Simonin *et al.*, 2020). Our results showed that the nodule microbiomes of plants inoculated with different soil suspensions varied significantly (Table S3). This difference is highlighted by soil 1 suspension-inoculated nodules being colonised by a range of *Mesorhizobium* ASVs and soil 2 suspension nodules almost colonised exclusively by *Mesorhizobium* ASV M.1 (Fig. 2). Also, plants grown in soil 1 suspension produced, on average, more nodules and had a broader range of shoot growth than those inoculated with soil 2 suspension (Figs 1, S2). However, the original soil suspensions inoculated onto the plants showed no differences in alpha diversity and only slight, although not significant, differences in beta diversity (Fig. S4; Table S3). The soils from which the suspensions were produced also had no noteworthy differences in their microbiome diversity or physicochemical properties (Fig. S4; Table S2). This suggests that lowly abundant soil microbes that do not sway diversity measures, may play a pivotal role in how the microbiome functions as a whole. Such a phenomenon has been described in peat soil, where a *Desulfosporosinus* sp., which comprised only 0.006% of the total microbiome, acted as an important sulphate reducer in the biogeochemical process that diverts carbon flow from methane to CO_2 (Pester *et al.*, 2010). Also, *Bacillus* species, typically found at a low abundance in the rhizosphere compared with rhizobia, increase the number of nodules and/or the size of nodules in legumes (Rajendran *et al.*, 2008; Mishra *et al.*, 2009; Schwartz *et al.*, 2013).

Starved *L. burttii* plant nodules harbour a microbiome different to that of healthy plants

Lotus burttii is the only species that we tested that showed a significant difference between the nodule microbiome of heathy and starved plants. Nodules of starved *L. burttii* plants were dominated by *Rhizobium* ASVs, while the nodules of healthy plants were predominantly colonised by *Mesorhizobium* ASVs. *Lotus burttii* is known to form infected but ineffective nodules upon inoculation with *Rhizobium leguminosarum* Norway, however this does not form nodules on *L. japonicus* or *L. corniculatus* (Gossmann *et al.*, 2012). This correlates with the observation that starved *L. japonicus* and *L. corniculatus* harboured nodules that were not dominated by *Rhizobium*, but rather by *Mesorhizobium*

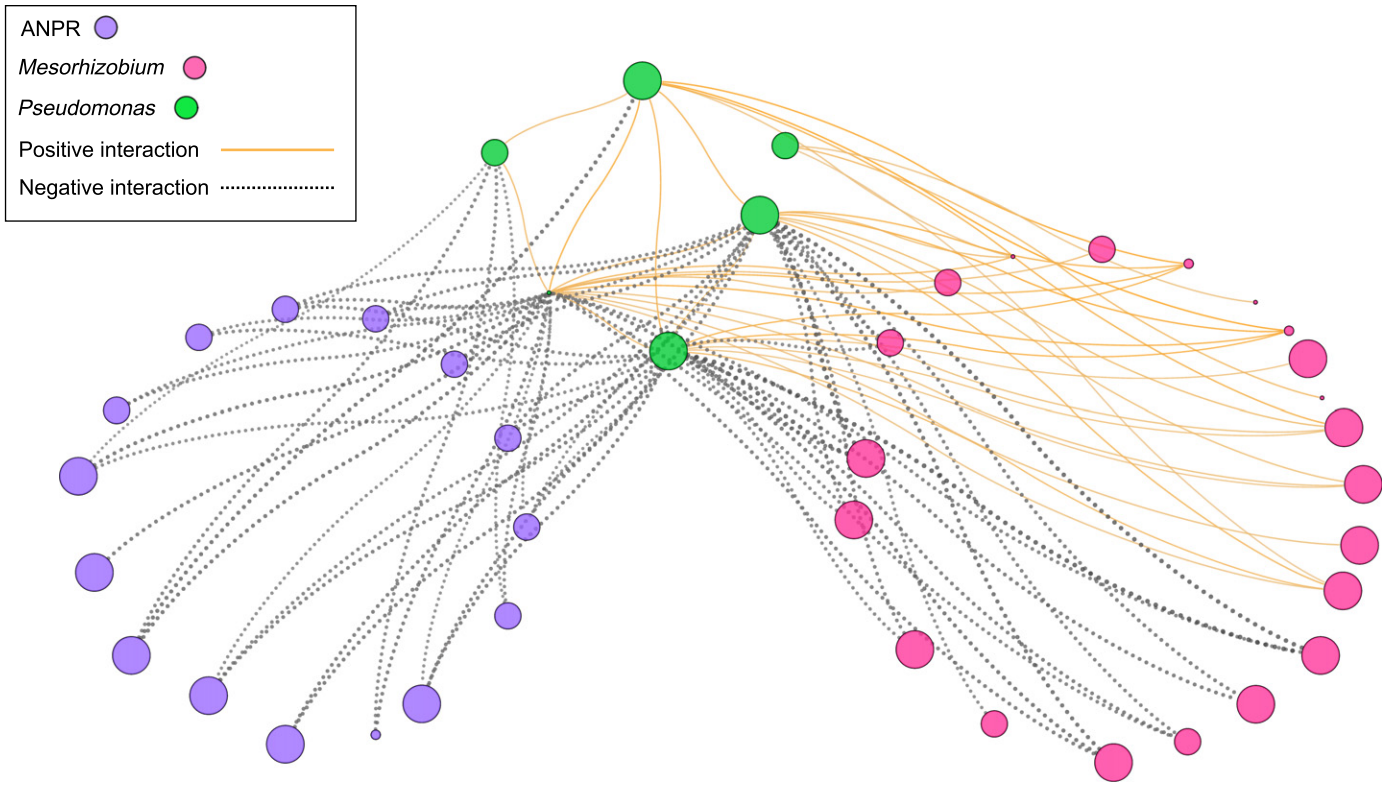

Fig. 4 Microbial co-occurrence network of *Lotus burttii*. An amplicon sequence variant (ASV) table of soil suspension 2-inoculated *L. burttii* samples was used to infer a correlation network SparCC (Friedman & Alm, 2012) algorithm implemented using the FastSpar (Watts *et al*., 2019) tool. The nodes (dots) of this network corresponding to ASVs are grouped and coloured by genus. Node size indicates the relative abundance. Each edge (line) between two ASVs represents either a positive (orange line) or negative (grey-dashed line) correlation. Only significant correlations ($|R| \geq 0.2$, $P < 0.01$) between Rhizobiaceae and Pseudomonadaceae families and first neighbours of Pseudomonadaceae are shown in the network.

ASVs, similar to the microbiome of healthy plants (Fig. 2). The variation in the starved-plant nodule microbiomes of *Lotus* species may be explained by how readily each plant is nodulated. Liang *et al.* (2019) described that ineffective *R. leguminosarum* Norway colonises nodules of *L. burttii* via cracks in the epidermis. *Lotus burttii* is more susceptible to less-specific infections (Zarrabian *et al.*, 2021), which is likely to increase its vulnerability to forming an ineffective symbiosis. This reduced specificity by *L. burttii* is also highlighted in the number of starved plants that contained nodules. In total, 73.8% of starved *L. burttii* plants grew nodules, much more than in *L. japonicus* and *L. corniculatus* (Fig. S2). The higher frequency of nodulation coupled with the reduced specificity that *L. burttii* exhibits in choosing a nodulation partner might leave the plant susceptible to expending energy on ineffective symbiotic processes, resulting in the starvation of the plant. Conversely, *L. corniculatus* and *L. japonicus* do not exhibit this same level of promiscuity, which is evidenced by their nodules being dominated by *Mesorhizobium* in all sample types. The reason as to why a starved plant would harbour a nodule microbiome similar to that of a healthy plant remains to be elucidated. We postulate that it may be simply a delay in the establishment of a successful symbiosis or due to being colonised by nonnitrogen-fixing *Mesorhizobium* strains. Rodpothong *et al.*, came to similar conclusions when inoculating *Mesorhizobium loti* Nod factor synthesis mutants onto different *Lotus* species. Nodulation of *L. burttii* was unaffected, while *L. japonicus* and *L. corniculatus* exhibited delayed nodulation and reduced infection (Rodpothong *et al.*, 2009). Taken together, our results support the idea that the reduced specificity exhibited by *L. burttii* during root–nodule symbiosis allows for a broader range of bacteria to colonise its nodules.

Pseudomonas ASVs are more prevalent in healthy *L. burttii* nodules and can reduce ineffective nodulation in *L. japonicus*

Although the microbiota of all nodule types were dominated by Rhizobiales bacteria, there was a small contingent of non-Rhizobiales ASVs detected as well (Fig. 2). This is not uncommon in legume nodules, as non-Rhizobiales bacteria are often isolated from nodules. Alphaproteobacteria, Betaproteobacteria, Gammaproteobacteria and Actinobacteria have all been found in various legumes nodules (Benhizia *et al.*, 2004; Dey *et al.*, 2004; Cummings *et al.*, 2009; Ibáñez *et al.*, 2009; Ampomah & Huss-Danell, 2011; Zhao *et al.*, 2013; Dobritsa & Samadpour, 2016; Ferchichi *et al.*, 2019). Of the non-rhizobia that were present in *Lotus* nodules, *Pseudomonas* was the most prevalent. We found that *Pseudomonas* ASVs were characteristic of healthy, but not of starved, *L. burttii* nodules (Fig. 3) suggesting that they have the potential to support plant health. Previous studies have shown that

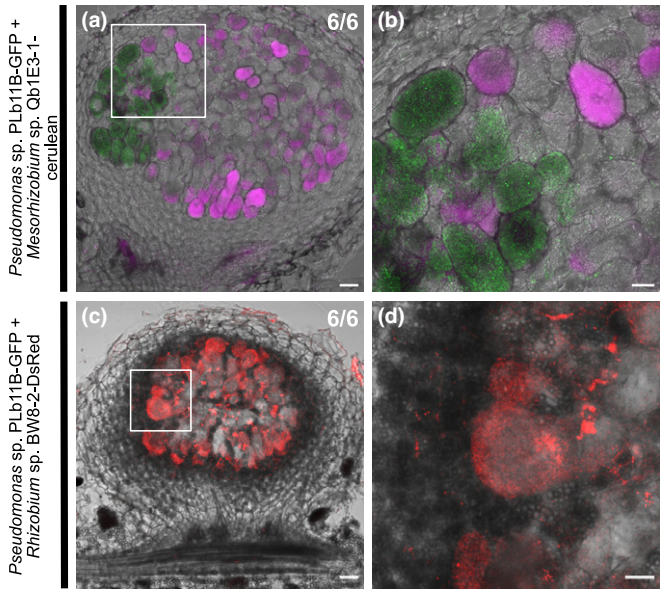

Fig. 5 *Pseudomonas* sp. PLb11B-GFP colonisation in nodules induced by *Mesorhizobium* sp. Qb1E3-1-cerulean and *Rhizobium* sp. BW8-2-DsRed. Nodules were prescreened for signs of fluorescence before sectioning. (a) Overview and (b) zoomed-in confocal microscopy image of *Pseudomonas* sp. PLb11B-GFP (green) and *Mesorhizobium* sp. Qb1E3-1-cerulean (magenta) colonisation in an effective *Lotus burttii* nodule. Overview image bar, 50 μm. Zoomed image bar, 20 μm. (c) Overview and (d) zoomed-in confocal microscopy image of *Pseudomonas* sp. PLb11B (green) and *Rhizobium* sp. BW8-2 (red) colonisation in an ineffective *L. burttii* nodule. Overview image bar, 50 μm. Zoomed image bar, 20 μm.

Pseudomonas can influence plant growth directly by producing siderophores, solubilising phosphate and producing indoleacetic acid (Dey *et al.*, 2004; Ibáñez *et al.*, 2009; Zhao *et al.*, 2013; Ferchichi *et al.*, 2019) or indirectly via antagonistic behaviour towards phytopathogenic fungi (Sindhu & Dadarwal, 2001; Chandra *et al.*, 2020). A *Pseudomonas* strain isolated from *Sophora alopecuroides* also promotes plant growth upon reinoculation with *Mesorhizobium* (Zhao *et al.*, 2013). We posit that potential microbe–microbe interactions involving *Pseudomonas* also influence the outcome of the root–nodule symbiosis. To analyse any potential microbe–microbe interactions within the nodules we looked for interactions between nodule ASVs. Network analysis comparing the nodule microbiome of healthy and starved *L. burttii* plants revealed significant negative correlations between *Pseudomonas* ASVs and multiple *Rhizobium* ASVs, as well as positive and negative interactions with *Mesorhizobium* ASVs (Fig. 4). These predicted interactions were supported by co-inoculating either an ineffective symbiont, *Rhizobium* sp. BW8-2, or an effective symbiont, *Mesorhizobium* sp. Qb1E3-1 with *Pseudomonas* sp. PLb11B. Each isolate had been previously isolated from *L. burttii* nodules, however it was found that *Pseudomonas* sp. PLb11B was only present in *Mesorhizobium*-induced nodules. Using fluorescently tagged strains and microscopy we found that 32.5% of nodules formed by the *Mesorhizobium* and 0% of nodules formed by *Rhizobium* contained *Pseudomonas*. *Pseudomonas* bacteria have been shown to colonise root hairs (Berggren *et al.*, 2005) or nodules intercellularly (Pastor-Bueis *et al.*, 2021). But in contrast, we found that *Pseudomonas* sp. PLb11B infection was intracellular and typically confined to small regions of each nodule with only a small number of cells showing extensive colonisation (Fig. 5). The lack of *Pseudomonas* sp. PLb11B in *Rhizobium* sp. BW8-2 induced nodules aligned with the sequencing data and interaction network observations. This negative interaction was further highlighted when observing another *Pseudomonas* isolate, Lb2C2, co-inoculated with *Rhizobium* sp. BW8-2 on *L. japonicus*. There was a significant reduction in the number of nodules and nodule primordia in *L. japonicus* compared with the single inoculation with the *Rhizobium* sp. BW8-2. Noticeably, this effect was host and inoculum specific, as no reduction in nodule number was observed in *L. burttii* or in co-inoculations of *Pseudomonas* with *Mesorhizobium* (Figs 6, S8). This contrasts with publications that suggested that *Pseudomonas* and *Rhizobium* strains interact synergistically (Tilak *et al.*, 2006; Egamberdieva *et al.*, 2010, 2013; Sánchez *et al.*, 2014). Interactions can be direct, for example filtrates from *Rhizobium* sp. increasing the cell density of *Pseudomonas fluorescens* (Samavat *et al.*, 2011), or mediated via the plant, for example indoleacetic acid produced by *Pseudomonas* sp. resulted in a more extensive root system in *Galega officinalis* and an increased number of potential infection sites for the compatible *Rhizobium* sp. (Egamberdieva *et al.*, 2013). The negative correlation we observed between *Pseudomonas* and *Rhizobium* ASVs in *L. burttii* nodules may also have been due to an indirect effect mediated by *Mesorhizobium*. Negative correlations were also seen between *Mesorhizobium* ASVs and *Rhizobium* ASVs. This can be explained by both bacteria competing for nodule colonisation. Significant positive correlations were apparent between *Pseudomonas* and *Mesorhizobium* ASV M.1, which was dominant in the healthy nodules of plants inoculated with soil suspension 2 (Fig. 2). Positive interactions have already been seen after the co-inoculation of *Pseudomonas* sp. isolates with a *Mesorhizobium* sp., which led to an increase in nodule number in chickpea (Malik & Sindhu, 2011). Positive correlations between *Mesorhizobium* and *Pseudomonas* coupled with the reduction in ineffective nodulation by cheater rhizobia upon co-inoculation with *Pseudomonas* supported the hypothesis that these *Pseudomonas* ASVs have a beneficial role in root–nodule symbiosis.

Our results add to the growing assertion that the soil microbiome, including non-Rhizobiales bacteria, greatly shape the overall functionality of root–nodule symbiosis and healthy plant growth (Martínez-Hidalgo & Hirsch, 2017). The ability for *Pseudomonas* to selectively colonise healthy plant nodules and reduce the number of ineffective nodules in *L. japonicus* indicated that root–nodule symbiosis is influenced by the broader soil microbiota. This research will aid the construction of synthetic communities capable of recreating observed patterns in a bid to narrow down which soil microbes and which microbe–microbe interactions are pivotal in forming the ideal microbiome to maximise plant growth.

Acknowledgements

We thank Juan Liang for help to isolate rhizobia strains, Anke Becker and Doreen Meier for providing the pABC-cerulean

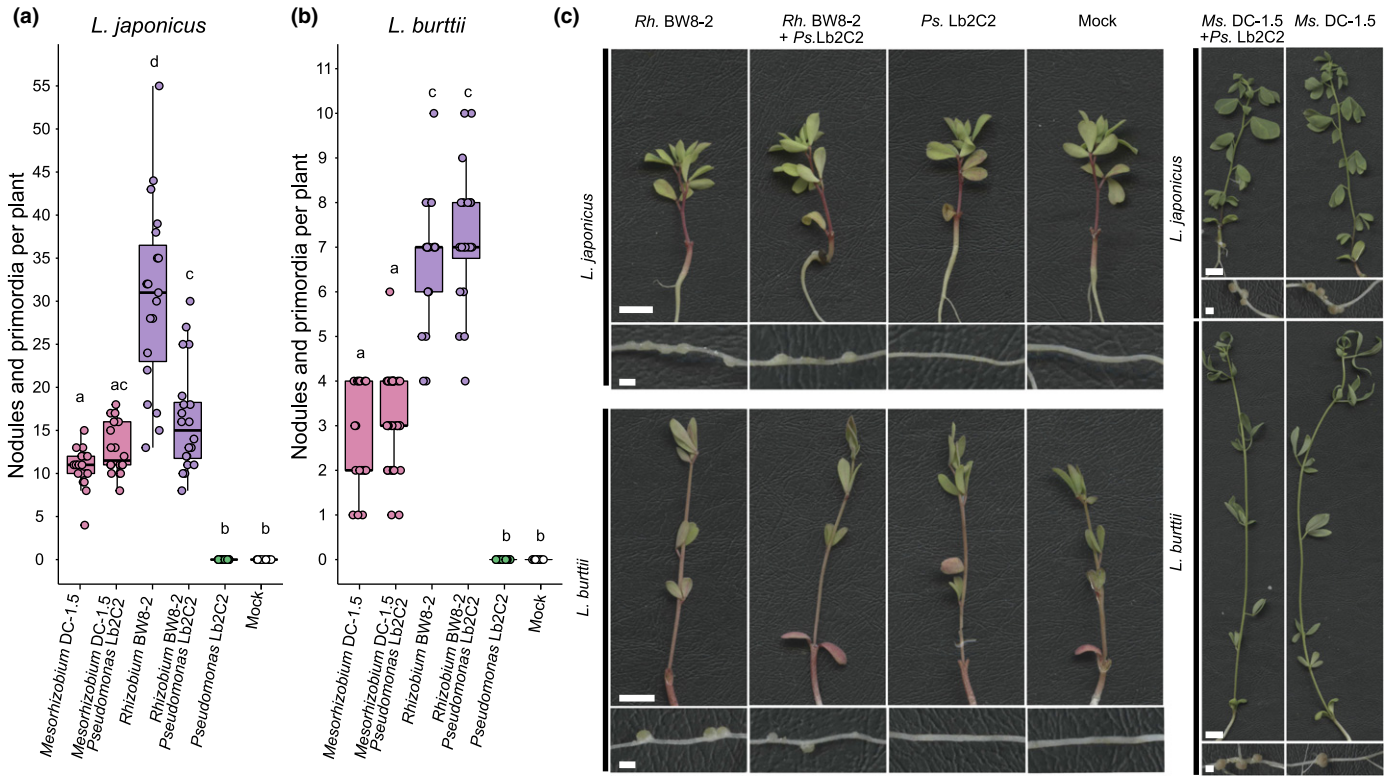

Fig. 6 Nodule organogenesis phenotype of *Lotus* plants inoculated with *Rhizobium* sp. BW8-2, *Mesorhizobium* sp. DC-1.5, and *Pseudomonas* sp. Lb2C2. Box plots of the number of nodules and nodule primordia formed on *Lotus japonicus* (a) and *Lotus burttii* (b) roots. In total, 20 plants were inoculated with *Rhizobium* sp. BW8-2, *Mesorhizobium* sp. DC-1.5 or *Pseudomonas* sp. Lb2C2 nodule isolates. *Lotus burttii* and *L. japonicus* were harvested at 4 and 5 wk post inoculation, respectively. Significance calculated using ANOVA and Tukey HSD is indicated as lowercase letters. Each point represents the number of nodules in one plant. The bold black line and the box depict the median and the interquartile range, respectively. (c) Representative images of root and shoot phenotypes of each inoculation treatment. Shoots bar, 5 mm. Nodules bar, 1 mm.

plasmid as well as Anna Beatrice Preinsberger and Oscar Gonzalez Puiggené for assisting in the construction of conjugated isolates. This work is supported by the German Research Foundation grants MA 7269/2-1 and Schl446/38-1. Open access funding enabled and organised by ProjektDEAL.

Author contributions

DBC and MMarín conceived and designed the study. DBC performed the experiments. DBC and MMahmoudi analysed the data. AB and VR performed MiSeq sequencing. EK and MS contributed with reagents and materials. DBC, MMarín and MMahmoudi contributed to writing and preparation of the manuscript. All authors read and approved the final manuscript.

ORCID

Andreas Brachmann https://orcid.org/0000-0001-7980-8173
Duncan B. Crosbie https://orcid.org/0000-0001-9917-1528
Eric Kemen https://orcid.org/0000-0002-7924-116X
Macarena Marín https://orcid.org/0000-0002-6966-2446
Viviane Radl https://orcid.org/0000-0001-6898-5430
Michael Schloter https://orcid.org/0000-0003-1671-1125

Data availability

All *16S* rRNA gene sequencing data were submitted to the Short Read Archive of NCBI and can be found under BioProject accession no. PRJNA731628. The data and scripts used for the machine learning and network analysis are available at https://github.com/IshtarMM/LotusNodules.

References

Altschul SF, Gish W, Miller W, Myers EW, Lipman DJ. 1990. Basic local alignment search tool. *Journal of Molecular Biology* **215**: 403–410.

Ampomah OY, Huss-Danell K. 2011. Genetic diversity of root nodule bacteria nodulating *Lotus corniculatus* and *Anthyllis vulneraria* in Sweden. *Systematic and Applied Microbiology* **34**: 267–275.

Bach HJ, Tomanova J, Schloter M, Munch JC. 2002. Enumeration of total bacteria and bacteria with genes for proteolytic activity in pure cultures and in environmental samples by quantitative PCR mediated amplification. *Journal of Microbiological Methods* **49**: 235–245.

Benhizia Y, Benhizia H, Benguedouar A, Muresu R, Giacomini A, Squartini A. 2004. Gamma proteobacteria can nodulate legumes of the genus *Hedysarum*. *Systematic and Applied Microbiology* **27**: 462–468.

Berggren I, Alström S, Van Vuurde J, Mårtensson AM. 2005. Rhizoplane colonisation of peas by *Rhizobium leguminosarum* bv. *viceae* and a deleterious *Pseudomonas putida*. *FEMS Microbiology Ecology* **52**: 71–78.

Bertani G. 1951. Studies on lysogenesis I: the mode of phage liberation by lysogenic *Escherichia coli*. *Journal of Bacteriology* **62**: 293–300.

Bray JR, Curtis JT. 1957. An ordination of the upland forest communities of southern Wisconsin. *Ecological Monographs* **27**: 326–349.

Brown SP, Grillo MA, Podowski JC, Heath KD. 2020. Soil origin and plant genotype structure distinct microbiome compartments in the model legume *Medicago truncatula*. *Microbiome* **8**: 1–17.

Callahan BJ, McMurdie PJ, Holmes SP. 2017. Exact sequence variants should replace operational taxonomic units in marker-gene data analysis. *The ISME Journal* **11**: 2639–2643.

Callahan BJ, McMurdie PJ, Rosen MJ, Han AW, Johnson AJA, Holmes SP. 2016. DADA2: high-resolution sample inference from Illumina amplicon data. *Nature Methods* **13**: 581–583.

Chandra H, Kumari P, Bisht R, Prasad R, Yadav S. 2020. Plant growth promoting *Pseudomonas aeruginosa* from *Valeriana wallichii* displays antagonistic potential against three phytopathogenic fungi. *Molecular Biology Reports* **47**: 6015–6026.

Cummings SP, Gyaneshwar P, Vinuesa P, Farruggia FT, Andrews M, Humphry D, Elliott GN, Nelson A, Orr C, Pettitt D. 2009. Nodulation of *Sesbania* species by *Rhizobium* (*Agrobacterium*) strain IRBG74 and other rhizobia. *Environmental Microbiology* **11**: 2510–2525.

Cytryn E. 2013. The soil resistome: the anthropogenic, the native, and the unknown. *Soil Biology and Biochemistry* **63**: 18–23.

Dey R, Pal K, Bhatt D, Chauhan S. 2004. Growth promotion and yield enhancement of peanut (*Arachis hypogaea* L.) by application of plant growth-promoting rhizobacteria. *Microbiological Research* **159**: 371–394.

Dobritsa AP, Samadpour M. 2016. Transfer of eleven species of the genus *Burkholderia* to the genus *Paraburkholderia* and proposal of *Caballeronia* gen. nov. to accommodate twelve species of the genera *Burkholderia* and *Paraburkholderia*. *International Journal of Systematic and Evolutionary Microbiology* **66**: 2836–2846.

Dorn-In S, Bassitta R, Schwaiger K, Bauer J, Hölzel CS. 2015. Specific amplification of bacterial DNA by optimized so-called universal bacterial primers in samples rich of plant DNA. *Journal of Microbiological Methods* **113**: 50–56.

Downie JA. 2005. Legume haemoglobins: symbiotic nitrogen fixation needs bloody nodules. *Current Biology* **15**: R196–R198.

Egamberdieva D, Berg G, Lindström K, Räsänen LA. 2010. Co-inoculation of *Pseudomonas* spp. with *Rhizobium* improves growth and symbiotic performance of fodder galega (*Galega orientalis* Lam.). *European Journal of Soil Biology* **46**: 269–272.

Egamberdieva D, Berg G, Lindström K, Räsänen LA. 2013. Alleviation of salt stress of symbiotic *Galega officinalis* L. (goat's rue) by co-inoculation of *Rhizobium* with root-colonizing *Pseudomonas*. *Plant and Soil* **369**: 453–465.

Ferchichi N, Toukabri W, Boularess M, Smaoui A, Mhamdi R, Trabelsi D. 2019. Isolation, identification and plant growth promotion ability of endophytic bacteria associated with lupine root nodule grown in Tunisian soil. *Archives of Microbiology* **201**: 1333–1349.

Friedman J, Alm EJ. 2012. Inferring correlation networks from genomic survey data. *PLoS Computational Biology* **8**: e1002687.

Gamborg OL, Miller RA, Ojima K. 1968. Nutrient requirements of suspension cultures of soybean root cells. *Experimental Cell Research* **50**: 151–158.

Gossmann JA, Markmann K, Brachmann A, Rose LE, Parniske M. 2012. Polymorphic infection and organogenesis patterns induced by a *Rhizobium leguminosarum* isolate from *Lotus* root nodules are determined by the host genotype. *New Phytologist* **196**: 561–573.

Graves S, Piepho H-P, Selzer ML. 2015. *Package 'MULTCOMPVIEW'. Visualizations of paired comparisons*. [WWW document] URL https://cran.r-project.org/web/packages/multcompView/multcompView.pdf [accessed 14 July 2021].

Gu S, Wei Z, Shao Z, Friman V-P, Cao K, Yang T, Kramer J, Wang X, Li M, Mei X *et al.* 2020. Competition for iron drives phytopathogen control by natural rhizosphere microbiomes. *Nature Microbiology* **5**: 1002–1010.

Han Q, Ma Q, Chen Y, Tian B, Xu L, Bai Y, Chen W, Li X. 2020. Variation in rhizosphere microbial communities and its association with the symbiotic efficiency of rhizobia in soybean. *The ISME Journal* **14**: 1915–1928.

Hansen BL, Pessotti RdC, Fischer MS, Collins A, El-Hifnawi L, Liu MD, Traxler MF. 2020. Cooperation, competition, and specialized metabolism in a simplified root nodule microbiome. *mBio* **11**: e01917-20.

Herrera-Cervera JA, Caballero-Mellado J, Laguerre G, Tichy H-V, Requena N, Amarger N, Martínez-Romero E, Olivares J, Sanjuan J. 1999. At least five rhizobial species nodulate *Phaseolus vulgaris* in a Spanish soil. *FEMS Microbiology Ecology* **30**: 87–97.

Howieson JG, Yates RJ, O'Hara GW, Ryder M, Real D. 2005. The interactions of *Rhizobium leguminosarum* biovar *trifolii* in nodulation of annual and perennial *Trifolium* spp. from diverse centres of origin. *Australian Journal of Experimental Agriculture* **45**: 199–207.

Ibáñez F, Angelini J, Taurian T, Tonelli ML, Fabra A. 2009. Endophytic occupation of peanut root nodules by opportunistic *Gammaproteobacteria*. *Systematic and Applied Microbiology* **32**: 49–55.

Kelly SJ, Muszyński A, Kawaharada Y, Hubber AM, Sullivan JT, Sandal N, Carlson RW, Stougaard J, Ronson CW. 2013. Conditional requirement for exopolysaccharide in the *Mesorhizobium-Lotus* symbiosis. *Molecular Plant–Microbe Interactions* **26**: 319–329.

Kereszt A, Mergaert P, Kondorosi E. 2011. Bacteroid development in legume nodules: evolution of mutual benefit or of sacrificial victims? *Molecular Plant–Microbe Interactions* **24**: 1300–1309.

Kramina TE, Degtjareva GV, Samigullin TH, Valiejo-Roman CM, Kirkbride J, Joseph H, Volis S, Deng T, Sokoloff DD. 2016. Phylogeny of *Lotus* (Leguminosae: Loteae): partial incongruence between nrITS, nrETS and plastid markers and biogeographic implications. *Taxon* **65**: 997–1018.

Liang J, Klingl A, Lin Y-Y, Boul E, Thomas-Oates J, Marín M. 2019. A subcompatible rhizobium strain reveals infection duality in *Lotus*. *Journal of Experimental Botany* **70**: 1903–1913.

Liu F, Hewezi T, Lebeis SL, Pantalone V, Grewal PS, Staton ME. 2019. Soil indigenous microbiome and plant genotypes cooperatively modify soybean rhizosphere microbiome assembly. *BMC Microbiology* **19**: 1–19.

Malik DK, Sindhu SS. 2011. Production of indole acetic acid by *Pseudomonas* sp.: effect of coinoculation with *Mesorhizobium* sp. *Cicer* on nodulation and plant growth of chickpea (*Cicer arietinum*). *Physiology and Molecular Biology of Plants* **17**: 25–32.

Marcos-García M, Menéndez E, Cruz-González X, Velázquez E, Mateos PF, Rivas R. 2015. The high diversity of *Lotus corniculatus* endosymbionts in soils of northwest Spain. *Symbiosis* **67**: 11–20.

Martin M. 2011. CUTADAPT removes adapter sequences from high-throughput sequencing reads. *Embnet.Journal* **17**: 10–12.

Martínez-Hidalgo P, Hirsch AM. 2017. The nodule microbiome: N_2-fixing rhizobia do not live alone. *Phytobiomes* **1**: 70–82.

McMurdie PJ, Holmes S. 2013. PHYLOSEQ: an R package for reproducible interactive analysis and graphics of microbiome census data. *PLoS ONE* **8**: e61217.

Mishra PK, Mishra S, Selvakumar G, Kundu S, Shankar GH. 2009. Enhanced soybean (*Glycine max* L.) plant growth and nodulation by *Bradyrhizobium japonicum-SB1* in presence of *Bacillus thuringiensis-KR1*. *Acta Agriculturae Scandinavica Section B – Soil and Plant Science* **59**: 189–196.

Noble WS. 2006. What is a support vector machine? *Nature Biotechnology* **24**: 1565–1567.

Oksanen J, Blanchet FG, Kindt R, Legendre P, Minchin P, O'hara R, Simpson G, Solymos P, Stevens MHH, Wagner H. 2018. *Community ecology package*. R package v.2.5-2. [WWW document] URL https://CRAN.R-project.org/package=vegan [accessed 22 April 2020].

Pastor-Bueis R, Jimenez-Gomez A, Barquero M, Mateos PF, González-Andrés F. 2021. Yield response of common bean to co-inoculation with *Rhizobium* and *Pseudomonas* endophytes and microscopic evidence of different colonised spaces inside the nodule. *European Journal of Agronomy* **122**: 126187.

Pedregosa F, Varoquaux G, Gramfort A, Michel V, Thirion B, Grisel O, Blondel M, Prettenhofer P, Weiss R, Dubourg V. 2011. SCIKIT-LEARN: machine learning in PYTHON. *The Journal of Machine Learning Research* **12**: 2825–2830.

Pester M, Bittner N, Deevong P, Wagner M, Loy A. 2010. A 'rare biosphere' microorganism contributes to sulfate reduction in a peatland. *The ISME Journal* **4**: 1591–1602.

Quast C, Pruesse E, Yilmaz P, Gerken J, Schweer T, Yarza P, Peplies J, Glöckner FO. 2012. The SILVA ribosomal RNA gene database project: improved data processing and web-based tools. *Nucleic Acids Research* **41**: D590–D596.

Rajendran G, Sing F, Desai AJ, Archana G. 2008. Enhanced growth and nodulation of pigeon pea by co-inoculation of *Bacillus* strains with *Rhizobium* spp. *Bioresource Technology* **99**: 4544–4550.

Remigi P, Zhu J, Young JPW, Masson-Boivin C. 2016. Symbiosis within symbiosis: evolving nitrogen-fixing legume symbionts. *Trends in Microbiology* **24**: 63–75.

Rodpothong P, Sullivan JT, Songsrirote K, Sumpton D, Cheung KW-T, Thomas-Oates J, Radutoiu S, Stougaard J, Ronson CW. 2009. Nodulation gene mutants of *Mesorhizobium loti* R7A—*nodZ* and *nolL* mutants have host-specific phenotypes on *Lotus* spp. *Molecular Plant–Microbe Interactions* **22**: 1546–1554.

Sachs JL, Simms EL. 2008. The origins of uncooperative rhizobia. *Oikos* **117**: 961–966.

Samavat S, Besharati H, Behboudi K. 2011. Interactions of rhizobia cultural filtrates with *Pseudomonas fluorescens* on bean damping-off control. *Journal of Agricultural Science and Technology* **13**: 965–976.

Sánchez AC, Gutiérrez RT, Santana RC, Urrutia AR, Fauvart M, Michiels J, Vanderleyden J. 2014. Effects of co-inoculation of native *Rhizobium* and *Pseudomonas* strains on growth parameters and yield of two contrasting *Phaseolus vulgaris* L. genotypes under Cuban soil conditions. *European Journal of Soil Biology* **62**: 105–112.

Sandal N, Jin H, Rodriguez-Navarro DN, Temprano F, Cvitanich C, Brachmann A, Sato S, Kawaguchi M, Tabata S, Parniske M. 2012. A set of *Lotus japonicus* Gifu× *Lotus burttii* recombinant inbred lines facilitates map-based cloning and QTL mapping. *DNA Research* **19**: 317–323.

Sandman K, Ecker C. 2014. *Pseudomonas* isolation and identification: an introduction to the challenges of polyphasic taxonomy. *Journal of Microbiology & Biology Education* **15**: 287–291.

Schumpp O, Deakin WJ. 2010. How inefficient rhizobia prolong their existence within nodules. *Trends in Plant Science* **15**: 189–195.

Schwartz A, Ortiz I, Maymon M, Herbold C, Fujishige N, Vijanderan J, Villella W, Hanamoto K, Diener A, Sanders E *et al.* 2013. *Bacillus simplex*—a little known PGPB with anti-fungal activity—alters pea legume root architecture and nodule morphology when coinoculated with *Rhizobium leguminosarum* bv. *viciae*. *Agronomy* **3**: 595–620.

Seefeldt LC, Hoffman BM, Dean DR. 2009. Mechanism of Mo-dependent nitrogenase. *Annual Review of Biochemistry* **78**: 701–722.

Shannon P, Markiel A, Ozier O, Baliga NS, Wang JT, Ramage D, Amin N, Schwikowski B, Ideker T. 2003. Cytoscape: a software environment for integrated models of biomolecular interaction networks. *Genome Research* **13**: 2498–2504.

Simonin M, Dasilva C, Terzi V, Ngonkeu EL, Diouf D, Kane A, Béna G, Moulin L. 2020. Influence of plant genotype and soil on the wheat rhizosphere microbiome: evidences for a core microbiome across eight African and European soils. *FEMS Microbiology Ecology* **96**: fiaa067.

Sindhu S, Dadarwal K. 2001. Chitinolytic and cellulolytic *Pseudomonas* sp. antagonistic to fungal pathogens enhances nodulation by *Mesorhizobium* sp. *Cicer* in chickpea. *Microbiological Research* **156**: 353–358.

Streeter JG. 1994. Failure of inoculant rhizobia to overcome the dominance of indigenous strains for nodule formation. *Canadian Journal of Microbiology* **40**: 513–522.

Thiergart T, Durán P, Ellis T, Vannier N, Garrido-Oter R, Kemen E, Roux F, Alonso-Blanco C, Ågren J, Schulze-Lefert P *et al.* 2020. Root microbiota assembly and adaptive differentiation among European *Arabidopsis* populations. *Nature Ecology & Evolution* **4**: 122–131.

Tilak K, Ranganayaki N, Manoharachari C. 2006. Synergistic effects of plant-growth promoting rhizobacteria and *Rhizobium* on nodulation and nitrogen fixation by pigeonpea (*Cajanus cajan*). *European Journal of Soil Science* **57**: 67–71.

Töwe S, Wallisch S, Bannert A, Fischer D, Hai B, Haesler F, Kleineidam K, Schloter M. 2011. Improved protocol for the simultaneous extraction and column-based separation of DNA and RNA from different soils. *Journal of Microbiological Methods* **84**: 406–412.

Tyc O, van den Berg M, Gerards S, van Veen JA, Raaijmakers JM, De Boer W, Garbeva P. 2014. Impact of interspecific interactions on antimicrobial activity among soil bacteria. *Frontiers in Microbiology* **5**: 567.

Venado RE, Liang J, Marín M. 2020. Rhizobia infection, a journey to the inside of plant cells. *Advances in Botanical Research* **94**: 97–118.

Vincent JM. 1970. *A manual for the practical study of the root-nodule bacteria*. Oxford, UK: Blackwell Scientific.

Wang D, Yang S, Tang F, Zhu H. 2012. Symbiosis specificity in the legume–rhizobial mutualism. *Cellular Microbiology* **14**: 334–342.

Watts SC, Ritchie SC, Inouye M, Holt KE. 2019. FastSpar: rapid and scalable correlation estimation for compositional data. *Bioinformatics* **35**: 1064–1066.

Werner D, Wilcockson J, Kalkowski B. 1975. Nitrogen fixing activity in separated from plant cell cultures. *Zeitschrift für Naturforschung C* **30**: 687–688.

Wickham H. 2009. Elegant graphics for data analysis. *Media* **35**: 10.1007.

William S, Feil H, Copeland A. 2012. Bacterial genomic DNA isolation using CTAB. *Sigma* **50**: 6876.

Winarno R, Lie T. 1979. Competition between *Rhizobium* strains in nodule formation: interaction between nodulating and non-nodulating strains. *Plant and Soil* **51**: 135–142.

Zarrabian M, Montiel J, Sandal N, Jin H, Lin YY, Klingl V, Marín M, James E, Parniske M, Stougaard J *et al.* 2021. A promiscuity locus confers *Lotus burttii* nodulation with rhizobia from five different genera. *bioRxiv*. doi: 10.1101/2021.08.26.457880.

Zgadzaj R, Garrido-Oter R, Jensen DB, Koprivova A, Schulze-Lefert P, Radutoiu S. 2016. Root nodule symbiosis in *Lotus japonicus* drives the establishment of distinctive rhizosphere, root, and nodule bacterial communities. *Proceedings of the National Academy of Sciences, USA* **113**: E7996–E8005.

Zhao LF, Xu YJ, Ma ZQ, Deng ZS, Shan CJ, Wei GH. 2013. Colonization and plant growth promoting characterization of endophytic *Pseudomonas chlororaphis* strain Zong1 isolated from *Sophora alopecuroides* root nodules. *Brazilian Journal of Microbiology* **44**: 629–637.

Supporting Information

Additional Supporting Information may be found online in the Supporting Information section at the end of the article.

Dataset S1 Metadata of all samples.

Fig. S1 Reproducibility of plant growth experiments.

Fig. S2 Number of nodules per plant after inoculation with soil suspensions.

Fig. S3 Rarefaction curves of sequencing data.

Fig. S4 Nodule microbiome alpha diversity plotted by species and soil suspension input.

Fig. S5 Global principal coordinate analysis of all samples.

Fig. S6 Overview network analysis.

Fig. S7 Root weight and shoot length phenotype of *Lotus* plants inoculated with *Rhizobium* sp. BW8-2, *Mesorhizobium* sp. DC-1.5, and *Pseudomonas* sp. Lb2C2.

Fig. S8 Nodule organogenesis phenotype of *Lotus* plants inoculated with *Rhizobium* sp. BW8-2, *Mesorhizobium* sp. DC-1.5, and *Pseudomonas* sp. Lb2C2.

Table S1 Strains and plasmids used.

Table S2 Physicochemical analysis of soil samples. h, humus soil; uL, silty clay.

Table S3 PERMANOVA analysis of beta diversity in all nodule microbiome sample types.

Please note: Wiley Blackwell are not responsible for the content or functionality of any Supporting Information supplied by the authors. Any queries (other than missing material) should be directed to the *New Phytologist* Central Office.